theoretical work designed to test directly these ideas is needed before a final picture emerges.

Acknowledgment. This work was supported by the Graduate School Research Fund of the University of Washington and NATO Fellowships to N.D.E. and F.B. N.D.E. is an A. P. Sloan Fellow (1976–1978).

References and Notes

(1) (a) Universitá di Bologna; (b) University of Washington.

(2) (a) F. Bernardi, I. G. Csizmadia, and N. D. Epiotis, *Tetrahedron*, **31**, 3085 (1975); (b) F. Bernardi, N. D. Epiotis, and R. Yates, *J. Am. Chem. Soc.*, **97**, 1334 (1975); (c) R. Yates, N. D. Epiotis, and F. Bernardi, *ibid.*, **97**, 4198 (1975); (d) N. D. Epiotis, R. Yates, and F. Bernardi, *ibid.*, **97**, 4198 (1975); (e) F. Bernardi, N. D. Epiotis, and R. Yates, *ibid.*, **97**, 6615 (1975).

(3) W. J. Hehre, W. A. Lathan, R. Ditchfield, M. D. Newton, and J. A. Pople, Program No. 236, Quantum Chemistry Program Exchange, Indiana University, Bloomington, Ind.

(4) (a) W. J. Hehre, R. F. Stewart, and J. A. Pople, *J. Chem. Phys.*, **51**, 2657 (1969); (b) R. Ditchfield, W. J. Hehre, and J. A. Pople, *ibid.*, **54**, 725 (1971).

(5) W. A. Lathan, L. A. Curtiss, W. J. Hehre, J. B. Lisle, and J. A. Pople, *Prog. Phys. Org. Chem.*, **11**, 175 (1974).

(6) S. Samdal and H. M. Seip, *J. Mol. Struct.*, **28**, 193 (1975).

(7) N. D. Epiotis, W. R. Cherry, S. Shaik, R. L. Yates, and F. Bernardi, *Top. Curr. Chem.*, **70** (1977).

(8) M. Wolfsberg and L. Helmholz, *J. Chem. Phys.*, **20**, 837 (1952).

(9) As is shown in Table V, the trend of the overlap integrals depends on the basis set, while the trend in the H_{ij}'s is not basis set dependent.

(10) (a) "Ionization Potentials, Appearance Potentials, and Heats of Formation of Gaseous Positive Ions", National Bureau of Standards, NBS 26, 1969; (b) A. D. Baker and D. Betteridge, "Photoelectron Spectroscopy", Pergamon Press, Elmsford, N.Y., 1972.

(11) See K. Fukui, *Acc. Chem. Res.*, **4**, 57 (1971); G. Klopman, Ed., "Chemical Reactivity and Reaction Paths", Wiley-Interscience, New York, N.Y., 1974; R. F. Hudson, *Angew. Chem., Int. Ed. Engl.*, **12**, 36 (1973).

(12) The quantities $(H_{ij}/\delta\epsilon)^2$ or $(H_{ij}/\delta\epsilon^2)$ and $H_{ij}^2/\delta\epsilon$ involve the interaction matrix element and the energy gap factors acting in competition. However, the balance in this competition is different in the two quantities. Accordingly, solutions may exist where indices related to $(H_{ij}/\delta\epsilon)^2$ or $(H_{ij}/\delta\epsilon)$ vary in one manner, while the indices related to $(H_{ij}^2/\delta\epsilon)$ vary by exactly the opposite manner. Our computations show that the relative ordering of F and Cl and well as OH and SH remains unaltered in all indices in all systems examined.

(13) H. Volz and W. D. Mayer, *Justus Liebigs Ann. Chem.*, 835 (1975); G. A. Olah, Y. K. Mo, and Y. Halpern, *J. Am. Chem. Soc.*, **94**, 551 (1972).

(14) (a) S. G. Lias, J. R. Eyler, and P. Ausloos, *Int. J. Mass Spectrom. Ion Phys.*, **19**, 219 (1976); (b) J. R. Eyler, P. Ausloos, and S. G. Lias, *J. Am. Chem. Soc.*, **96**, 3673 (1974).

(15) G. S. Hammond, *J. Am. Chem. Soc.*, **77**, 334 (1955).

(16) The fact that sulfur might be a better π donor than oxygen in certain excited states of some organic compounds was pointed out by Mangini; see A. Mangini and R. Passerini, *Gazz. Chim. Ital.*, **84**, 606 (1954); A. Mangini, *Rev. Chim.*, **1**, 313 (1962); A. Mangini, *Mem. Accad. Lincei*, in press.

(17) H. C. Brown and R. R. Holmes, *J. Am. Chem. Soc.*, **78**, 2173 (1956).

(18) J. M. Miller and M. Onyszchuk, *Can. J. Chem.*, **42**, 518 (1964); E. Gore and S. S. Danyluk, *J. Phys. Chem.*, **69**, 89 (1965).

(19) R. G. Pearson, "Hard and Soft Acids and Bases", Dowden, Hutchinson, and Ross, Stroudsburg, Pa., 1973; R. G. Pearson, *J. Chem. Educ.*, **45**, 581 (1968).

(20) G. Klopman and R. F. Hudson, *Theor. Chim. Acta*, **8**, 165 (1967).

Stereoelectronic Properties of Photosynthetic and Related Systems. 1. Ab Initio Quantum Mechanical Ground State Characterization of Free Base Porphine, Chlorin, and Ethyl Pheophorbide *a*

Dale Spangler,[1,2] Gerald M. Maggiora,*[3] Lester L. Shipman,[4] and Ralph E. Christoffersen*[1]

Contribution from the Departments of Chemistry and Biochemistry, University of Kansas, Lawrence, Kansas 66045, and the Chemistry Division, Argonne National Laboratory, Argonne, Illinois 60439.

Received December 30, 1976

Abstract: Ab initio SCF calculations on the ground state of free base porphine, chlorin, and ethyl pheophorbide *a* have been carried out using the molecular fragment procedure. Molecular orbital energies and ordering, and the correlations of specific orbitals among the molecules studied, have been examined in detail. Ionization potentials have been estimated, and the first ionization potentials are 6.8, 6.4, and 6.4 eV for porphine, chlorin, and ethyl pheophorbide *a*, respectively. The calculations show the expected approximate separation of the HOMO, HOMO − 1, LUMO, and LUMO + 1 from the remainder of the MO manifold in keeping with the "four orbital" model, and isodensity contour plots of occupied and unoccupied molecular orbitals indicate a striking similarity in the "shapes" of these orbitals in all three molecules. Charges and bond orders have been examined. In porphine and chlorin, the bonding picture includes an extended π system whose path of conjugation involves the atoms of the interior of the macrocycle, including the nitrogens and methine carbons. Also, relatively localized π bonds are found between the exterior carbon atoms of the pyrrole moieties. In ethyl pheophorbide *a*, the π bonds of the keto carbonyl of ring V and the vinyl group of ring I are mostly localized, but the path of conjugation within the macrocycle is somewhat less clear. Finally, molecular electrostatic isopotential maps have been constructed and an analysis of the long-range electrostatic field and its relationship to intermolecular interactions is discussed.

Photosynthesis involving either plants or bacteria is well known to be one of the most important energy-conversion mechanisms carried out by living systems. In converting solar to chemical energy and in maintaining the oxygen balance in our biosphere, photosynthesis plays a crucial role. Hence, a detailed understanding of the primary processes that govern photosynthetic energy conversion is of great importance, both to an understanding of fundamental biological processes and to the development of alternate energy sources based on biomimetic conversion of solar energy.

Chlorophyll molecules play a central role in the primary events[5] of photosynthesis. The majority of chlorophyll molecules act cooperatively as an antenna to absorb light and funnel the electronic excitation energy to a "reaction center", where charge separation occurs involving a few special chlorophyll molecules.[6] Although much is now known about the role of chlorophyll in photosynthetic energy conversion, there is still little known about the geometric arrangement and collective electronic structure of associated chlorophyll molecules in the photosynthetic membrane.

The studies described in this and the following paper represent the beginning of a series[7] of investigations, using ab initio quantum mechanical and other theoretical techniques, whose goals are to elucidate the salient electronic and geometric structural features of monomeric and aggregated chlorophyll systems, and to relate these features to the functions of chlorophyll in photosynthetic energy conversion. The current studies characterize several monomers of interest related to chlorophyll, by examining various electronic structural features of the ground states of these molecules. In particular, this paper reports ab initio SCF-MO studies using the molecular fragment method[8] on free base porphine (162 electrons), chlorin (164 electrons), and ethyl pheophorbide *a* (330 electrons). The companion paper following in this issue describes analogous studies on the corresponding magnesium-containing species, i.e., magnesium porphine (172 electrons), magnesium chlorin (174 electrons), and ethyl chlorophyllide *a* (340 electrons). These ab initio studies provide, for the first time, an approximate but complete (i.e., including all σ and π electrons) description of the ground state electronic structure of these important molecules. These studies represent also (in terms of numbers of electrons) the largest nonpolymeric molecular systems examined to date using ab initio techniques. The discussion will focus on the similarities and differences among these molecules, in order to elucidate at least some of the features that make chlorophyll so uniquely suited for photosynthetic energy conversion. These studies will also provide a basis for subsequent studies of spectral properties and oligomeric structure.

Porphyrins have been studied by molecular orbital techniques for over 25 years.[9,10] Most of these studies have been by semiempirical techniques, and they recently have been reviewed.[11] One of the molecules included in the present study, free base porphine, has been studied previously by an ab initio technique.[12]

Methodology

The various magnesium-free molecules included in this study are depicted in Figure 1. The ab initio molecular fragment technique[8] using floating spherical Gaussian orbitals (FSGO) was employed in all calculations, and the basis orbitals used for describing the various C, N, O, and H environments were those recommended on the basis of earlier studies of prototype systems.[13]

The resulting description is then characterized in terms of molecular orbitals (MO):

$$\varphi_i = \sum_{s}^{N} c_{si} G_s \qquad s = 1, 2, \ldots, N \tag{1}$$

where N is the number of FSGO basis functions (G_s) used in the calculation. Also of interest in describing the charge distribution are several other quantities, including the charge and bond order matrix ($\mathbf{P}$), defined by

$$\mathbf{P}_{st} = 2 \sum_{i}^{\text{occ}} c_{si} c_{ti} \tag{2}$$

where the sum is over all occupied molecular orbitals, and its analogue ($\mathbf{P}'$) in a symmetrically orthogonalized basis,[14,15] defined by

$$\mathbf{P}' = \mathbf{S}^{1/2}\mathbf{P}\mathbf{S}^{1/2} \tag{3}$$

where $\mathbf{S}$ is the overlap matrix over the various FSGO basis orbitals.

In the symmetrically orthogonalized basis, the diagonal elements of $\mathbf{P}'$ are interpreted as electron populations, and hence give direct information about the charge distribution of the molecule. The off-diagonal elements are interpreted as bond orders, and are taken as measures of the strength and degree of bond localization.

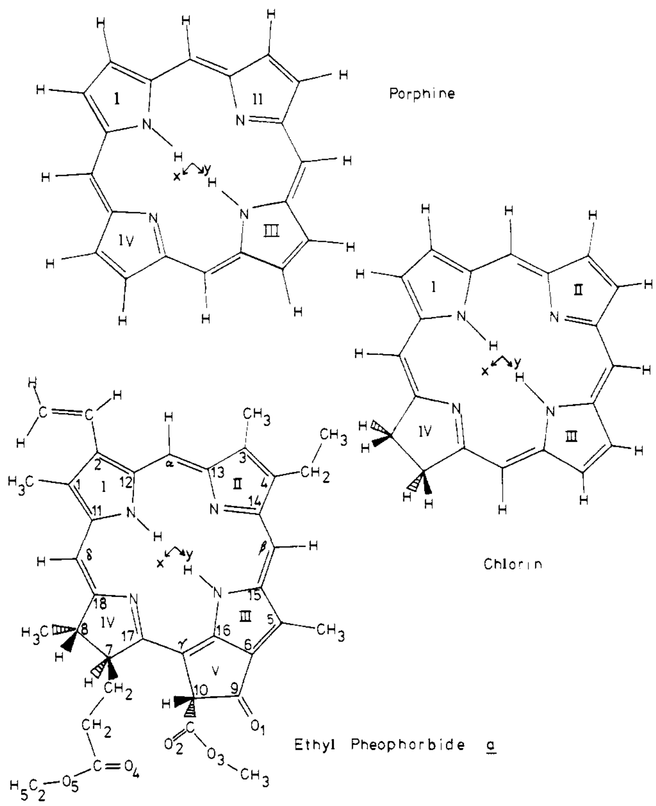

Figure 1. Free base molecules included in this study. Only one of several possible resonance structures is shown for convenience. The atom numbering for each of the molecules is illustrated for ethyl pheophorbide, and N_1, N_2, N_3, and N_4 are associated with rings I, II, III, and IV, respectively.

Another measure of interest to questions of chemical reactivity is the molecular electrostatic potential [$U(\mathrm{r})$], which is given by

$$U(\mathrm{r}) = \sum_{\alpha}^{M} \frac{Z_\alpha}{|\mathrm{r} - \mathbf{R}_\alpha|} - \int d\mathrm{r}_1 \rho(1)/|\mathrm{r} - \mathrm{r}_1| \tag{4}$$

where M is the number of nuclei, Z_α is the charge on the nucleus α, $\mathbf{R}_\alpha$ is the position of nucleus α, and $\rho(1)$ is the electron density calculated from the wave function.

Finally, correlation of MOs from one molecule to another requires special care, owing both to the low symmetry possessed by most of the molecules and to the large number of basis functions that typically contribute to a given MO. In order to systematize the correlation of MOs between molecules, the following measure was found to be particularly useful:[16]

$$\tau_{ij}^2 = \left| \sum_{s} (c_{si})^{\mathrm{A}} (c_{sj})^{\mathrm{B}} \right|^2 \tag{5}$$

In the above expression, $(c_{si})^{\mathrm{A}}$ represents the sth coefficient of the ith MO of molecule A in a symmetrically orthogonalized basis.[14] Since the size of the basis sets for the molecules A and B will not in general be the same, the symetrically orthogonalized basis for the molecule having the smaller number of basis functions is augmented with $c_{si} = 0$ until the basis set sizes coincide. Then, either if the overlap of basis functions common to both MOs is small, or if the basis functions not common to both molecules dominate the MO description, τ_{ij}^2 will be small. Hence, τ_{ij}^2 is a measure of the degree to which the ith MO of molecule A resembles the jth MO of molecule B, and provides a systematic and quantitative measure of the degree of MO similarity (i.e., correlation) between molecules.

The nuclear geometries were taken from available x-ray crystallographic data, with slight idealization as appropriate. In particular, the porphine ring geometry was taken basically

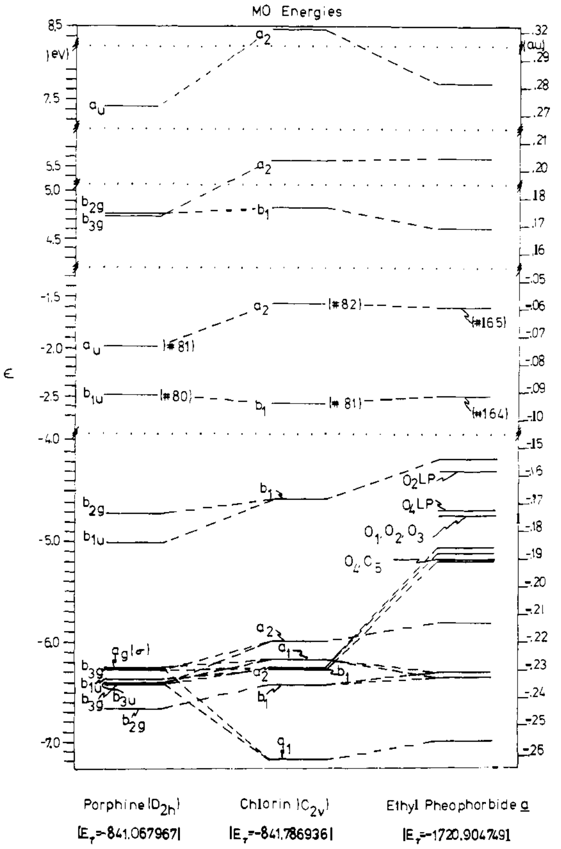

Figure 2. Molecular orbital energies of several high-lying occupied and low-lying unoccupied orbitals of three magnesium-free species related to chlorophyll. Note that, owing to the slight out-of-plane skewing brought about by reduction of the C_7–C_8 double bond in porphine, the C_{2v} symmetry in chlorin is only approximate. Except where indicated, all molecular orbitals are π-type orbitals. All MOs with negative energy are filled and all those with positive energy are unfilled. MO correlations are indicated by dashed lines. All correlations with $\tau_{ij}^2 \geq 0.25$ (see eq 5) are included in the figure. Orbitals labeled [O] are mixtures of π and lone pair basis functions located on the oxygens. Total energies (in Hartree atomic units) are also given for each molecule for reference purposes.

from the x-ray study of Webb and Fleischer,[17] using the idealization suggested by Almlöf[12] in an earlier study of porphine. The coordinates of chlorin were idealized from those of porphine, taking appropriate account of the effect of bond length changes in the C_7–C_8 bond.[18] The x-ray studies of Fischer et al.[19] were used to obtain coordinates for ethyl pheophorbide *a*. The atomic Cartesian coordinates used in this study are available upon request.

Results and Discussion

In describing the similarities and differences among the free base species, several different kinds of quantities calculable from wave function and energetic data can lead to significant insights into the chemical and physical properties related to electronic structure. These features include MO energies, MO electron density contours, electron populations, bond orders, and molecular isopotential maps. In the following sections, each of these properties will be discussed and related to available experimental data.

Molecular Orbital Energies. In Figure 2, the energies for several high-lying filled and low-lying unfilled MOs of porphine, chlorin, and ethyl pheophorbide *a* are given, along with the corresponding MO correlations.

One of the interesting questions that can be addressed as a result of the present ab initio studies is how well the "four-orbital model"[20] remains valid as more substituents and rings are added to the porphyrin macrocycle. In terms of energetics, we see from Figure 2 that, at least for porphine and chlorin, the four orbitals of interest (MOs 80–83 in porphine and 81–84 in chlorin) remain relatively well isolated from the remaining filled and virtual MOs. It is of interest to note that a switch in ordering occurs in the lowest unoccupied MO in going from porphine to chlorin. In fact, only in porphine is the unoccupied MO of b_{2g} symmetry the lowest unoccupied MO. In all other cases, the MOs that correlate to the b_{2g} LUMO in porphine become the LUMO + 1. However, since the LUMO and LUMO + 1 in porphine are nearly degenerate, the chemical and spectroscopic manifestations of the LUMO, LUMO + 1 ordering are not expected to be large.

In ethyl pheophorbide *a*, several additional complications occur. While the four basic orbitals can still be identified, the energetic separation between the HOMO −1 and HOMO − 2 as well as between the LUMO + 1 and LUMO + 2 is seen to be decreased substantially compared to the other molecules. In addition, the HOMO and LUMO in ethyl pheophorbide *a* show substantial contributions from substituents attached to the macrocycle (see below), thus changing the nature of the "four orbitals" as well as their energetics. This may have a significant effect on the ability of the four-orbital model to describe spectral features in ethyl pheophorbide *a*. This point is currently under further investigation.

Also of interest are correlations between MOs other than those involved in the four-orbital model. In making these correlations, all pairs of MOs having $\tau_{ij}^2 \geq 0.25$ have been connected. As expected, not all correlations have $\tau_{ij}^2 \sim 1$.[16] So that the degree of correlation can be understood, the various calculated τ_{ij}^2 are given in Table I. As seen in this table, some of the correlations are obviously unique (e.g., MO 80 in porphine to MO 81 in chlorin), but other correlations are much less so (e.g., MO 74 in porphine to MOs 74 and 78 in chlorin).

Among the interesting points related to these correlations is the appearance of new MOs which occur when the number of electrons is increased. In chlorin, there is one more filled MO than in porphine, and the extra orbital can be thought of as arising from a breaking of one π bond and forming two C–H bonds. This results in the disappearance of a high-lying π MO in chlorin, and the subsequent splitting of many porphine π MOs in going to chlorin. The new C–H bonds formed in chlorin contribute to MOs that are low in energy compared to the HOMO. In going to ethyl pheophorbide *a* the situation is substantially more complex, owing to the increase in the number of filled MOs (82 to 165). Of particular interest is the appearance of various MOs having substantial contributions from O_2 and O_4. Also, O_1 contributes to the HOMO and LUMO (see below), but MOs associated with O_3 and O_5 lie lower in energy.

Summarizing these correlations, the MOs of the four-orbital model correlate straightforwardly, and do not include other MOs. For the lower lying MOs, the lack of symmetry in ethyl pheophorbide *a* and relatively close spacing allows substantial splitting to occur, but MO correlations can be followed, nevertheless, using the quantitative measure τ_{ij}^2.

Another item of interest displayed in Figure 2 is the relationship among the ionization potentials and other calculated MO energies. Only one other ab initio calculation on any of the molecules included in our study has been carried out,[12] and in that study a basis set of 426 atomic Gaussians was contracted to an effective basis set of 136 functions in the study of porphine. In the current study, a basis of 144 FSGO was contracted to 120 functions for use at the SCF level. While many of the features of the MO energy spectrum calculated using the two basis sets are similar, several differences can be seen. First, virtual orbitals having negative orbital energies appear in the atomic GTO calculations,[12] making interpretation of MO energies in terms of ionization potentials difficult

Table I. Calculated Correlations between Molecular Orbitals of the Free Base Molecules[a,b]

Porphine MO i	Chlorin MO j	τ_{ij}^2	Chlorin MO i	Ethyl pheophorbide *a* MO j	τ_{ij}^2
84	85	0.707	85	168	0.553
	84*	0.118		169	0.227
	52	0.059		170	0.100
83*	83*	0.985	84*	167*	0.919
82*	84*	0.788	83*	166*	0.882
	52	0.050		169	0.043
	82	0.044			
81*	82*	0.912	82*	165*	0.882
80*	81*	0.989	81*	164*	0.933
79	80	0.558	80	163	0.883
	64	0.132			
	75	0.064			
	72	0.54			
	34	0.043			
78	80	0.440	79	155	0.769
	64	0.173			
	75	0.073			
	72	0.069			
	34	0.056			
77	78	0.561	78	153	0.587
	74	0.421		154	0.367
76	79	0.645	77	158	0.368
	77	0.307		159	0.320
				148	0.089
75	76	0.993	76	156	0.607
				159	0.101
				148	0.088
				149	0.067
74	74	0.548	75	154	0.522
	78	0.438		153	0.304
				155	0.052
73	77	0.689	74	152	0.903
	79	0.274			
72	75	0.857			
	64	0.050			

[a] See eq 5 for the method of calculating τ_{ij}^2. All $\tau_{ij}^2 \geq 0.04$ are included in the table. See ref 16 for additional discussion. [b] An asterisk denotes a four-orbital model MO.

Table II. Ionization Potential Estimates[a] for Free Base Porphine, Free Base Chlorin, and Ethyl Pheophorbide *a*

Molecule	Molecular orbital No.	Molecular orbital Type[b]	Ionization potential estimate, eV
Porphine	81	$a_u(\pi)$	6.8
	80	$b_{1u}(\pi)$	7.2
	79	$b_{3g}(\pi)$	9.2
	78	$b_{1u}(\pi)$	9.4
	77	$a_g(\sigma)$	10.5
Chlorin	82	$a_2(\pi)$	6.4
	81	$b_1(\pi)$	7.2
	80	$b_1(\pi)$	9.0
	79	$a_2(\pi)$	10.3
Ethyl pheophorbide *a*	165	π	6.4
	164	π	7.2
	163	π	8.7
	162	n[c]	8.8
	161	n[d]	9.1
	160	n, π[e]	9.2
	159	π	9.4
	158	π	9.5
	157	n, π[f]	9.5_6
	156	π	9.5_7
	155	π	10.1

[a] Ionization potential estimates given in the table are based upon the use of eq 6, the data from Figure 2, and Koopman's theorem (see ref 21). [b] Note that the MO type designation is only approximate in chlorin and ethyl pheophorbide *a* due to their nonplanarity. [c] Lone pair (O_2). [d] Lone pair (O_4). [e] Lone pair (O_3, O_1, O_2) + carbonyl π (O_2). [f] Lone pair (O_5) + carbonyl π (O_4).

using Koopman's theorem.[21] In addition, the ordering of the top two filled MOs is reversed in comparison to the results of the current study, with additional differences in ordering occurring among lower energy filled MOs. Incidentially, the ordering of the top two filled MOs found in the current study is the same as that found in an earlier CNDO/2 study.[22] Closer examination shows that the cases where ordering differences occur are primarily associated with MOs having a substantial contribution from N lone pairs e.g., b_{1u}). since it has been found that, for similar but simpler systems such as pyrrole, the MO ordering involving lone pair type MOs vs. other MOs was properly predicted using the molecular fragment basis[23] compared to an extended basis,[24] but was not correctly described using a minimum atomic GTO basis of the type used by Almlöf,[12] it appears that the MO ordering of the current study may be more appropriate for comparison to and/or prediction of experimental ionization potentials.

To allow comparison of calculated and observed ionization potentials, it is of interest to note first that, on the basis of earlier studies,[13] it is expected that the MO energies calculated using the molecular fragment basis should be linearly related to the values that would be found if an extended basis were used. Since an extended basis set study for molecules of this size is not feasible currently, examination of smaller systems having characteristics similar to those of the molecules studied here with extrapolation to the molecules of current interest is a reasonable alternative.

A suitable smaller molecule is the pyrrole molecule, where there are both chemical similarities to moieties present in the molecules studied here and extended basis sets available for comparison.[24] As expected, a least-squares comparison of the 13 filled valence MO energies calculated using the molecular fragment basis[23] (ϵ_{MF}) and using the extended basis[25] (ϵ_{ref}) gives rise to the linear relationship

$$\epsilon_{ref} = -0.1831 + 0.8852\epsilon_{MF} \tag{6}$$

with a correlation coefficient of 0.9995 and a standard deviation of 8×10^{-3}, where the values are given in atomic units.[26] If it is assumed that this relationship is applicable also to the systems studied here, the ionization potential estimates given in Table II can be obtained from the orbital energies given in Figure 2.

Since experimental ionization potential estimates using photoelectron or other techniques are not available generally for these systems, comparison of either trends or absolute values is not possible. For example, only one molecule has an estimated first ionization potential, i.e., free base porphine, where a value of 7.22 eV has been reported.[27] Our ionization potential estimates indicate that reasonable resolution of the first several ionization potentials (all from the respective π systems) can be expected for all three of these molecules. In addition, a "band-type" structure appearing at approximately 10 eV for porphine and chlorin would be expected, while in ethyl pheophorbide *a* considerably closer ionization potential spacing (e.g., in a photoelectron spectrum) would be expected in the 8–10-eV region.

Molecular Orbital Shapes. Owing to the significant role that the four-orbital model[20] has played in previous theoretical studies and in the rationalization of observed spectra, it is of interest to examine the shapes of these MOs in greater detail via electron density contour maps. In this way, the changes that occur in going from porphine to chlorin to ethyl pheophorbide

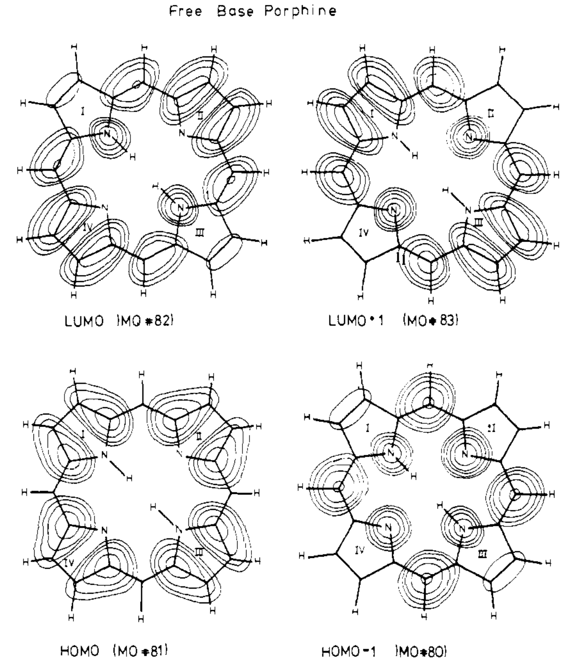

Figure 3. Electron density contour maps for the LUMO, LUMO + 1, HOMO, and HOMO − 1 of porphine. Contours are at levels of 10, 20, 40, 80, and 160 millielectrons/(Bohr)^3, and are constructed for a plane 1.0 Bohr above the macrocycle plane.

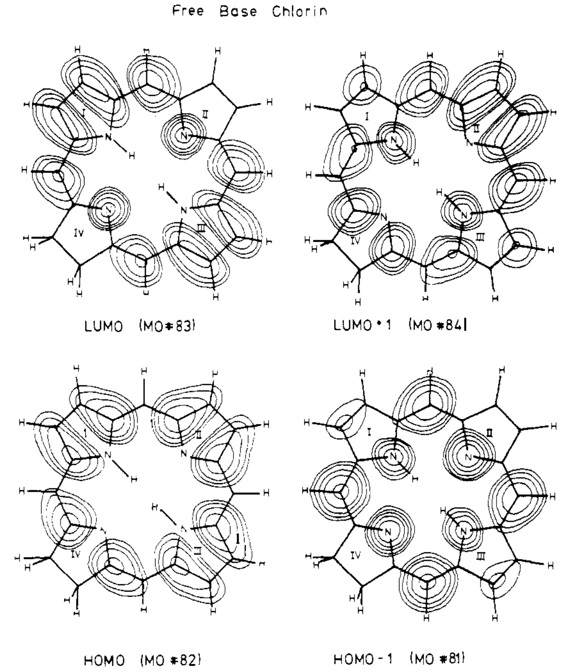

Figure 4. Electron density contour maps for the LUMO, LUMO + 1, HOMO, and HOMO − 1 of chlorin. Contours are at levels of 10, 20, 40, 80, and 160 millielectrons/(Bohr)^3, and are constructed for a plane 1.0 Bohr above the macrocycle plane.

a can be identified, along with the relevance of those changes to the applicability of the four-orbital model. Figures 3–5 give electron density contour maps for the two highest occupied, and hole density contour maps for the two lowest unoccupied, MOs of each of the three free base molecules studied.

Considering first the HOMO of the molecules we see that, comparing chlorin to porphine, the shape of the HOMO is nearly identical, except for the "local" effect that is seen in ring IV. In that region, a loss of delocalization in ring IV of chlorin due to reduction of the C_7–C_8 porphine double bond has taken place. Thus, the increase in energy of the HOMO in chlorin compared to that in porphine can be rationalized simply by a reduction in the extent of the π system in ring IV of chlorin, but with the overall shape of the HOMO being otherwise the same.

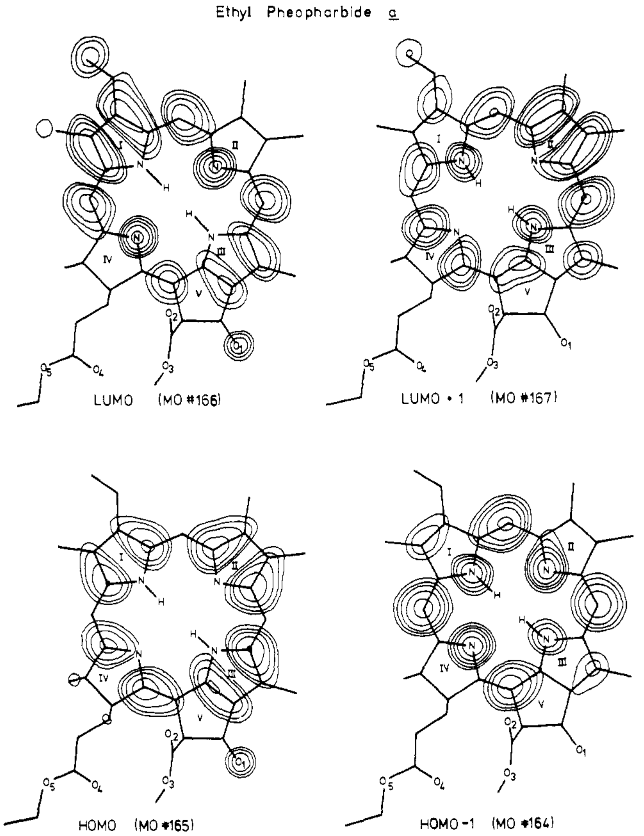

Figure 5. Electron density contour maps for the LUMO, LUMO + 1, HOMO, and HOMO −1 of ethyl pheophorbide *a*. Contours are at levels of 10, 20, 40, 80, and 160 millielectrons/(Bohr)^3, and are constructed for a plane 1.0 Bohr above the plane containing approximately all four nitrogen nuclei.

Comparing ethyl pheophorbide *a* to chlorin, we see that, even though substantial chemical changes have occurred, including addition of a fifth ring and a variety of substituents to the macrocycle, the basic shape of the HOMO in both cases is quite similar. The exception is that, in ethyl pheophorbide *a*, a contribution from O_1 to the HOMO is observed. While this apparently has little effect on the energy of the HOMO in these two molecules, the contribution of O_1 is nonnegligible, and may have an effect on electronic spectra and other properties of chlorophyll systems.

Comparing next the HOMO − 1 in each molecule, it is seen that, both in terms of shape and of energy, this MO is nearly identical in the three molecules.

In the cases of the LUMO and LUMO + 1, one point of interest is the change in ordering of MOs in going from porphine to chlorin, where the LUMO in porphine becomes the LUMO + 1 in chlorin. In addition, the LUMO + 1 in chlorin shows some hole density redistribution compared to the LUMO in porphine, not only in ring IV where the bond saturation has taken place, but also in rings I and III. This density redistribution is accompanied also by a substantial energetic destabilization. In going from chlorin to ethyl pheophorbide *a*, however, very few changes in density distribution or energy occur in the LUMO + 1.

For the LUMO + 1 in porphine, which becomes the LUMO in chlorin and ethyl pheophorbide *a*, very little change is seen in going from porphine to chlorin, either in the density distri-

Table III. Electron Populations and Bond Orders for the π Orbitals of Free Base Porphine and Free Base Chlorin

Free base porphine	Free base chlorin
Populations	
N_2: 1.173	N_2: 1.144
C_{14}: 1.004	C_{14}: 1.049
C_4: 1.025	C_4: 1.039
C_β: 1.102	C_β: 1.056
C_{15}: 1.005	C_{15}: 1.044
C_5: 1.032	C_5: 1.008
N_3: 1.491	N_3: 1.502
	C_6: 1.067
	C_{16}: 0.963
	C_γ: 1.199
	C_{17}: 0.997
	N_4: 1.096
Bond Orders[a]	
N_2–C_4: −0.211	N_2–C_4: −0.218
N_2–C_{14}: 0.611	N_2–C_{14}: 0.615
C_4–C_{14}: 0.355	C_4–C_{14}: 0.384
C_{13}–C_β: −0.214	C_{13}–C_β: −0.203
C_3–C_4: 0.866	C_3–C_4: 0.848
C_{14}–C_β: 0.591	C_{14}–C_β: 0.567
C_β–C_{15}: 0.605	C_β–C_{15}: 0.636
C_{15}–C_5: 0.451	C_{15}–C_5: 0.452
C_{15}–N_3: 0.529	C_{15}–N_3: 0.490
C_5–C_6: 0.810	C_5–C_6: 0.806
C_5–N_3: −0.200	C_5–N_3: −0.220
C_{16}–N_3: 0.529	C_{16}–N_3: 0.560
	C_6–C_{16}: 0.456
	C_{16}–C_γ: 0.566
	C_γ–C_{17}: 0.627
	C_{17}–N_4: 0.629

[a] All π-bond orders ≥ |0.2| are given.

Table IV. Electron Populations and Bond Orders for the π Orbitals of Ethyl Pheophorbide *a*

		Populations		
N_2: 1.166	N_3: 1.488	O_2: 1.165	O_4: 1.149	N_1: 1.527
C_{14}: 1.048	C_6: 1.088	C_γ: 1.155	C_δ: 1.214	C_{2a}: 0.968
C_4: 1.040	C_{16}: 0.977	C_{17}: 1.030	C_{11}: 0.955	C_{2b}: 1.047
C_β: 1.042	C_9: 1.066	N_4: 1.078	C_1: 1.065	C_α: 1.115
C_{15}: 1.088	O_1: 1.010	C_{18}: 0.999	C_2: 1.002	C_{13}: 1.022
C_5: 1.040	C_{10a}: 1.140	C_{7c}: 1.148	C_{12}: 1.007	C_3: 1.076

	Bond Orders[a] Macrocycle Only	
N_2–C_4: −0.251	C_6–C_{16}: 0.489	N_1–C_{11}: 0.533
N_2–C_{14}: 0.546	N_3–C_6: −0.205	C_1–C_2: 0.784
C_4–C_{14}: 0.362	C_{16}–C_γ: 0.496	C_2–C_{12}: 0.379
C_{13}–C_β: −0.248	C_γ–C_{17}: 0.674	C_α–C_{12}: 0.693
C_3–C_4: 0.818	C_{17}–N_4: 0.566	N_1–C_{12}: 0.482
C_{14}–C_β: 0.647	N_4–C_{18}: 0.694	C_{13}–C_α: 0.495
C_β–C_{15}: 0.562	C_δ–C_{18}: 0.554	C_3–C_{13}: 0.383
C_{15}–C_5: 0.547	C_{18}–C_γ: −0.266	N_2–C_{13}: 0.383
C_{15}–N_3: 0.459	C_δ–C_{11}: 0.627	N_2–C_3: −0.200
C_5–C_6: 0.694	C_δ–C_α: 0.205	C_9–C_6: 0.291
C_5–N_3: −0.221	N_1–C_δ: −0.202	
C_{16}–N_3: 0.597	C_1–C_{11}: 0.409	

Macrocycle-Peripheral Substituent Bond Orders			
C_{2a}–C_2: 0.310	C_{2b}–C_1: −0.241	C_{2b}–C_{2a}: 0.946	O_1–C_9: 0.934

[a] Bond orders involving peripheral substituents only have been omitted. All other π-type bond orders ≥ |0.2| are given.

bution or energetically. In the transition to ethyl pheophorbide *a*, however, new contributions from O_1 and the vinyl group at C_2 are seen. These contributions, which serve to enlarge the size of the π system, result in a stabilization of the LUMO in ethyl pheophorbide *a*.

Hence, while the MOs of the four-orbital model remain somewhat separated energetically from the others, at least for porphine and chlorin, changes in the density distribution are seen in several cases, including new contributions from O_1 and/or the vinyl group at C_2. In addition, the changes in density distribution appear to be related in a straightforward manner to the energetic changes that are observed.

Electron Populations and Bond Orders. In addition to understanding the nature of individual MOs, it is of interest to examine the *total* charge distribution, to compare the similarities and differences in the three molecules studied. To achieve this, π-electron populations and bond orders for each of the three molecules are given in Tables III and IV, using a symmetrically orthogonalized basis formed from the original FSGO basis[14,14] to present the results (see eq 3). It should also be noted that the entries in these tables obviously do not represent all possible populations and bond orders. Instead, the entries are a compromise, designed to allow discussion of relevant chemistry without inundating the reader with numbers.

Considering the σ-type electron populations and bond orders first, we found that few changes in these populations occur in going from porphine to chlorin to ethyl pheophorbide *a*. Therefore, we have not included these σ populations and bond orders in Tables III and IV, and we will not discuss them further.

In the case of π-type populations and bond orders, significant changes are seen, owing to the greater ease of polarization of electrons in this type of MO. In porphine, for example, the two types of nitrogens, which have substantial resemblance to pyrrole- and pyridine-type nitrogens, show significant differences in their π-electron populations, with N_2 (and N_4) having a smaller π population than N_1 (and N_3). It is also of interest to note that the methine π population ($C_\alpha = C_\beta = C_\gamma = C_\delta$) in porphine is greater than in any of the other carbon atoms, implying a greater susceptibility with respect to electrophilic attack. Comparing these porphine π populations to other molecules, it is seen that in chlorin the reduction of ring IV produces asymmetries in the π-electron charge distribution. For example, C_4 and C_6 are no longer equivalent, nor are N_2 and N_4. In addition, C_γ (and C_δ) becomes more π-electron rich than C_α (and C_β). The C_γ and C_δ methine positions are especially electron rich (1.199 electrons) for carbon atoms, and this correlates well with the observation[28] that the methine positions are especially susceptible to electrophilic attack. Rings I, II, and III, and the methine positions as a group all gain electrons in going from porphine to chlorin, while ring IV loses electrons.

In ethyl pheophorbide *a*, the π populations of the nitrogens decrease in the order $N_4 < N_2 < N_3 < N_1$, and the relatively low N_4 population is consistent with the qualitative suggestion made earlier[29] in which reduced pyrrole units are considered to have less tendency to "pull" electrons from the methine bridges and, therefore, should have less negative charge on the nitrogen. Also, the methine carbons now have π populations in the order $C_\delta > C_\alpha > C_\beta$. This suggests that the deuterium exchange rates may be different for each of these positions. As in the case of chlorin, the C_δ position is especially π-electron rich. This is consistent with experimental determination of the pseudo-first-order exchange rate[30] from ^{1}H NMR, where the rates at C_α, C_β, and C_δ are all much less than 5×10^{-8} s^{-1}, but exchange at C_δ is observed under acidic conditions. This redistribution is also reflected elsewhere in the π system where, for example, the π population at C_{11} is further reduced compared to chlorin, and becomes the lowest π population of all. Also, the vinyl group shows the expected asymmetry, with the π population of C_{2b} greater than that of C_{2a}. The vinyl group is also considerably localized, with a bond order of 0.946, but

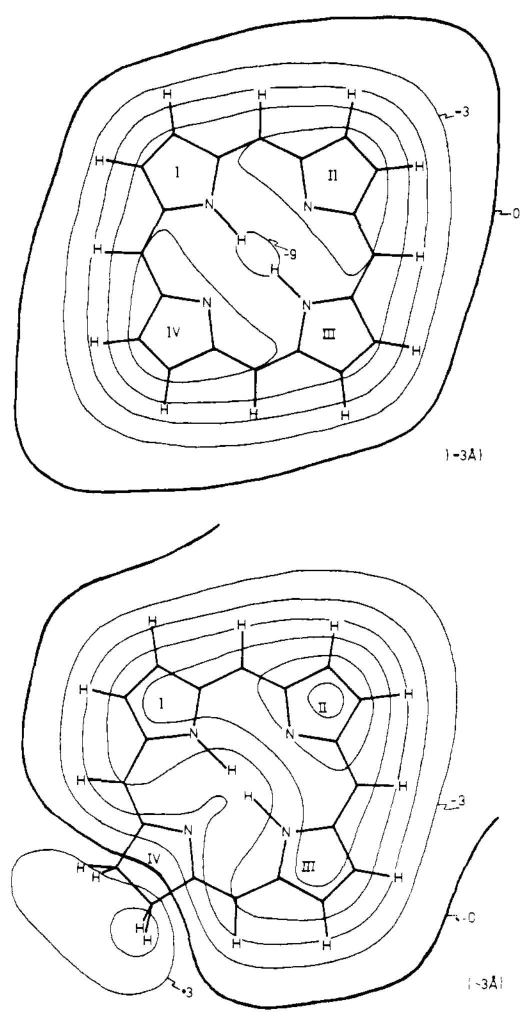

Figure 6. Electrostatic isopotential maps for free base porphine and chlorin constructed in a plane 3.0 Å below the macrocycle plane. Contour levels are given in kcal/mol, and are in increments of 3 kcal/mol.

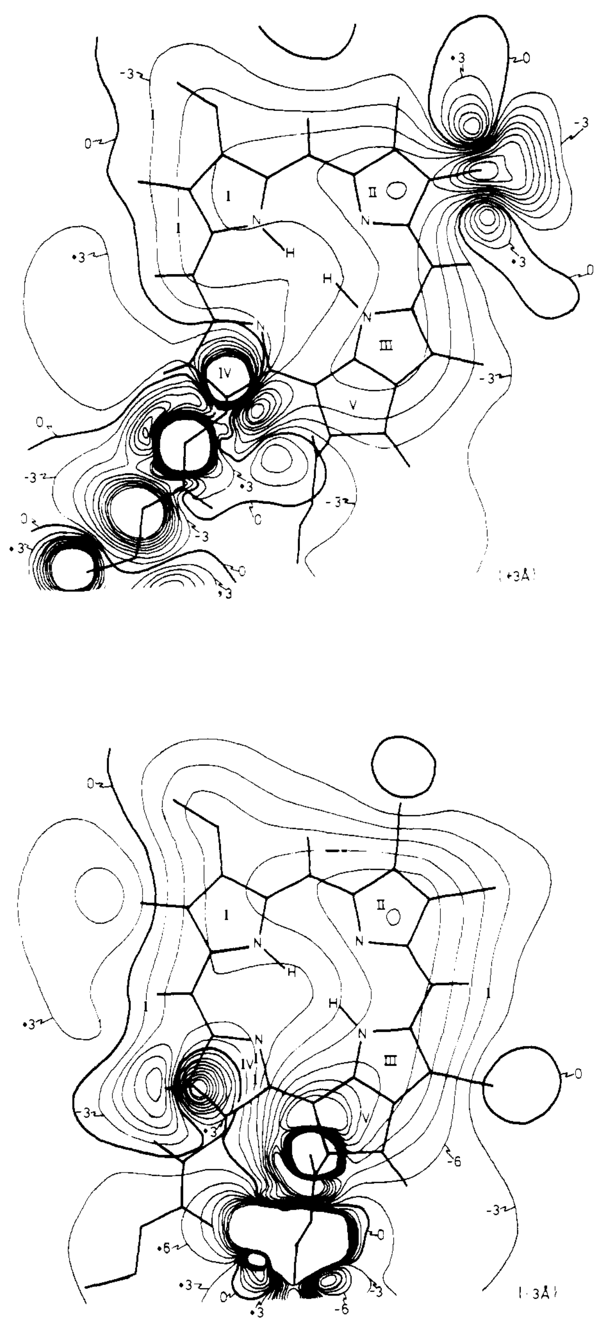

Figure 7. Electrostatic isopotential maps for ethyl pheophorbide *a*, constructed in planes ±3.0 Å from a plane containing approximately all four nitrogen nuclei. Contour levels are given in kcal/mol and are in increments of 3 kcal/mol.

nevertheless is conjugated to the macrocycle π system via a C_{2a}–C_2 π-bond order of 0.310.

Considering next the π-bond orders in the various molecules, several additional electronic structural features of interest can be discerned. In porphine, for example, we note first that the C_3–C_4 and C_5–C_6 π-bond orders are quite high, especially when compared to the bond orders connecting other adjacent atoms (e.g., C_4–C_{14}). In addition, N_2–C_{14}, C_{14}–C_β, C_β–C_{15}, C_{15}–N_3, etc., π-bond orders are all within the range 0.525–0.650. This suggests that, of the several possible resonance structures that might be proposed for porphine, the two resonance structures that most closely correspond to the observed bond orders are A and B. Four localized π bonds are found in resonance structure A, and two localized bonds are found in resonance structure B. The other π electrons are delocalized over the remainder of the macrocycle. The above resonance pathways, which have been proposed previously for porphine,[17] correspond to stable aromatic systems of 14 and 18 π electrons, respectively, and are consistent with the Huckel "4*n* + 2" rule.[10]

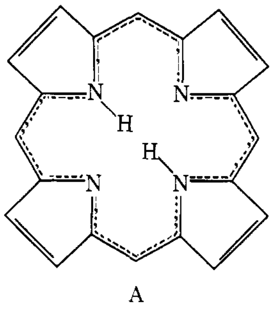

A

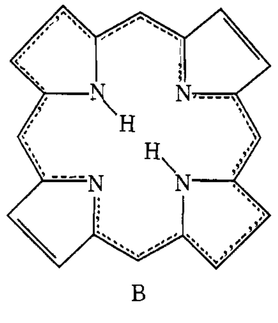

B

Proceeding to chlorin, it is expected that reduction of the C_7–C_8 bond should be possible without major disruption of the remaining π system. As is seen in Table III, this does occur, with localized π bonds remaining at C_1–C_2, C_3–C_4, and C_5–C_6 as measured by the large bond orders between symmetrically orthogonalized basis functions on these pairs of atoms. Also, the N_2–C_{14}, C_{14}–C_β, and C_β–C_{15} bond orders are again within the range 0.525–0.650, and the C_{15}–N_3 bond order is 0.490, supporting the notion that the remaining π electrons are delocalized about the macrocycle. Thus, few changes from porphine are observed.

For the case of ethyl pheophorbide *a*, many similarities re-

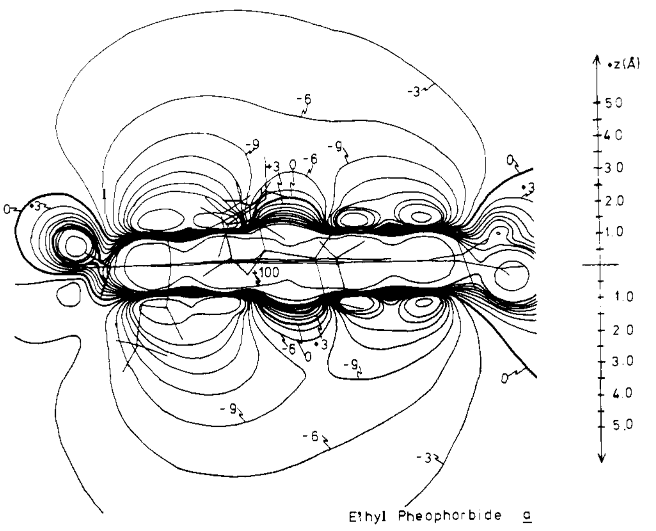

Figure 8. Electrostatic isopotential map for ethyl pheophorbide *a* constructed in the *yz* plane (see Figure 1). Contour levels are given in kcal/mol and are in increments of 3 kcal/mol.

main, but several significant differences in π-bond orders are seen. For example, the localized nature of the C_1–C_2, C_3–C_4, and C_5–C_6 bonds, while still discernible (at least for C_1–C_2 and C_3–C_4), is much less clear. In addition, the π electrons that were viewed as being delocalized over the macrocycle in porphine and chlorin are seen now to have a more localized character. For example, C_{12}–C_α, C_{13}–N_2, C_{14}–C_β, C_γ–C_{17}, N_4–C_{18}, and C_δ–C_{11} now have a more localized nature compared to N_1–C_{12}, C_α–C_{13}, N_2–C_{14}, etc. However, since the localized nature of these bonds is not nearly as clear as in the cases of porphine and chlorin, it does not seem appropriate to attempt to characterize ethyl pheophorbide *a* in terms of one or two resonance structures.

Several other features are also of interest. For example, as might be expected, no significant interactions between the side chains are seen in the π-bond orders. Although the vinyl and $C{=}O_1$ moieties show strong localized character (bond orders of 0.946 and 0.934, respectively), there are significant bond orders between C_2 and C_{2a} (0.310) and between C_6 and C_9 (0.291). Thus, both in terms of electron density contours and electron populations and bond orders, a significant role of both $C_9{=}O_1$ and the vinyl group is seen in the description of the electronic structure of ethyl pheophorbide *a*.

Electrostatic Isopotential Maps. To gain additional insight into questions of chemical reactivity and charge distribution, electrostatic isopotential maps have been prepared for each of the molecules using eq 4, as shown in Figures 6–8. In each figure, the convention is such that a negative contour indicates that a point positive charge located in the vicinity of the contour would experience an attractive potential. Also, it should be remembered that these isopotential maps provide only approximate measures of chemical reactivity, since they do not consider effects such as polarization or charge transfer that might occur in actual systems. However, they are expected to provide quite useful measures for the initial stages of chemical reactions and for long-range intermolecular interactions.

Considering the individual molecules, it is seen that porphine represents only an attractive potential for positively charged incoming species, with a slight preference indicated for rings II and IV over rings I and III. In the case of chlorin, a slight asymmetry in ring IV is seen. In addition, the region in the neighborhood of the reduced C_7–C_8 bond no longer presents an attractive potential, and the attractive region now becomes localized in ring II.

In the case of ethyl pheophorbide *a*, several additional effects are seen. First, the "sidedness" of the molecule that results from substituents pointing in different directions from the macrocycle is seen. In the region 3 Å above the macrocycle (i.e., the ethyl ester side), the attractive regions are seen around the region of the $C_{10a}{=}O_2$ moiety, outside ring IV, and in a rather wide area encompassing rings I, II, and III. In the region 3 Å below the macrocycle (i.e., the methyl ester side), attractive regions are seen near the O_5 ester type oxygen, in addition to generally nonspecific attractive regions in the vicinities of rings I, II, III, and V. These features are displayed in another perspective in Figure 8, where the somewhat nonspecific attractive regions are more easily seen.

Thus, through a variety of measures, a detailed comparison of similarities and differences among electronic structural features of porphine, chlorin, and ethyl pheophorbide *a* has been possible. In the following paper, these similarities and differences will be compared to the corresponding similarities and differences in the magnesium-containing analogues.

Acknowledgments. This work was supported in part by the Division of Physical Research, U.S. Energy Research and Development Administration. Partial support of some of the computing time required for this work by the University of Kansas is also gratefully acknowledged. We thank Dr. J. J. Katz for many helpful discussions, and Mr. Ross McKinney for help in the initial calculations.

References and Notes

(1) Department of Chemistry, University of Kansas.
(2) Participant in the Argonne Thesis Parts Program.
(3) Department of Biochemistry, University of Kansas.
(4) Argonne National Laboratory.
(5) For a recent review, see A. J. Bearden and R. Malkin, *Q. Rev. Biophys.*, **7**, 131–177 (1975).
(6) J. J. Katz and J. R. Norris, *Curr. Top. Bioenerg.*, **5**, 41–75 (1973).
(7) For a preliminary report on a portion of this work, see D. Spangler, R. McKinney, Jr., R. E. Christoffersen, G. M. Maggiora, and L. L. Shipman, *Chem. Phys. Lett.*, **36**, 427–431 (1975).
(8) See L. E. Nitzsche, C. Chabalowski, and R. E. Christoffersen, *J. Am. Chem. Soc.*, **98**, 4794–4801 (1976), and references contained therein, for a description of the molecular fragment method.
(9) H. Kuhn, *J. Chem. Phys.*, **17**, 1198–1212 (1949).
(10) W. T. Simpson, *J. Chem. Phys.*, **17**, 1218–1221 (1949).
(11) S. J. Chantrell, C. A. McAuliffe, R. W. Munn, and A. C. Pratt, *Coord. Chem. Rev.*, **16**, 259–284 (1975).
(12) J. Almlöf, *Int. J. Quantum Chem.*, **8**, 915–924 (1974).
(13) R. E. Christoffersen, D. Spangler, G. G. Hall, and G. M. Maggiora, *J. Am. Chem. Soc.*, **95**, 8526–8536 (1973).
(14) P. O. Löwdin, *J. Chem. Phys.*, **18**, 365–375 (1950).
(15) L. L. Shipman and R. E. Christoffersen, *Chem. Phys. Lett.*, **15**, 469–474 (1972).
(16) Generally, $\Sigma_j \tau_{ij}^2 \simeq 1$, where the *i*th MO belongs to one molecular species and the *j*th MO belongs to the other molecular species whose MOs are being correlated. The summation is taken over the set of MOs of the appropriate molecular species.
(17) L. E. Webb and E. B. Fleischer, *J. Am. Chem. Soc.*, **87**, 667–669 (1975). See also H. Kobayashi, *J. Chem. Phys.*, **30**, 1362, 1373 (1959); *Nippon Kagaku Zasshi*, **81**, 519 (1960); H. Kuhn, *Fortschr. Chem. Org. Naturst.*, **17**, 404 (1959); C. Weiss, H. Kobayashi, and M. Gouterman, *J. Mol. Spectrosc.*, **16**, 415 (1965).
(18) In order to reduce the strain in ring IV brought about by reduction of the C_7–C_8 bond, a slight out-of-plane twist of the C_7–C_8 bond is required.
(19) M. S. Fischer, D. H. Templeton, A. Zalkin, and M. Calvin, *J. Am. Chem. Soc.*, **94**, 3613–3619 (1972).
(20) M. Gouterman, G. Wagniere, and L. C. Snyder, *J. Mol. Spectrosc.*, **11**, 108–127 (1963).
(21) T. Koopmans, *Physica*, **1**, 104–113 (1933).
(22) G. M. Maggiora, *J. Am. Chem. Soc.*, **95**, 6555–6559 (1973).
(23) D. W. Genson and R. E. Christoffersen, *J. Am. Chem. Soc.*, **94**, 6904–6914 (1972).
(24) H. J. T. Preston and J. J. Kaufman, *Int. J. Quantum Chem.*, **S7**, 207–215 (1973). It might be noted that pyridine is also a smaller system having characteristics similar to those of the molecules studied here. However, the linear relationship for pyridine corresponding to eq 6 is quite similar to that for pyrrole (see ref 13), and the pyrrole parameters have been used for convenience.
(25) E. Clementi, H. Clementi, and D. R. Davis, *J. Chem. Phys.*, **46**, 4725–4730 (1967).
(26) Unless otherwise stated, all quantities reported will be given using Hartree atomic units. See H. Shull and G. G. Hall, **184**, 1559–1560 (1959).
(27) A. Stanieda, *Z. Naturforsch. B*, **23**, 1285–1295 (1968).
(28) R. B. Woodward and V. Skiric, *J. Am. Chem. Soc.*, **83**, 4676–4678 (1961).
(29) J.-H. Fuhrhop, *Struct. Bonding (Berlin)*, **18**, 1–67 (1974).
(30) R. C. Dougherty, H. H. Strain, and J. J. Katz, *J. Am. Chem. Soc.*, **87**, 104–109 (1965).